

All-silica fiber Bessel-like beam generator and its applications in longitudinal optical trapping and transport of multiple dielectric particles

Sung Rae Lee,¹ Jongki Kim,¹ Sejin Lee,¹ Yongmin Jung,² Jun Ki Kim,³ and K. Oh^{1*}

¹Institute of Physics and Applied Physics, Yonsei University, 262 Seongsanno, Seodaemun-gu, Seoul 120-749, Korea

²Optoelectronic Research Centre, University of Southampton Highfield, Southampton SO17 1BJ, UK

³Wellman Center for Photomedicine, Harvard Medical School, Massachusetts General Hospital
40 Blossom St. BAR 812, Boston, MA 02114, USA

*koh@yonsei.ac.kr

Abstract: A Bessel-like beam was generated in a novel all-fiber integrated structure. A concentric ring intensity pattern was achieved by the multimode interference along the coreless silica fiber, which was then focused by the integrated micro-lens to result in a Bessel-like beam. The average beam diameter of 7.5 μm maintained over 500 μm axial length for a continuous wave Yb-doped fiber laser input oscillating at the wavelength of 1.08 μm . The generated beam was successfully applied to two-dimension optical trapping and longitudinal transport of multiple dielectric particles confirming its unique non-diffracting and self-reconstructing nature. Physical principle of operation, fabrication, and experimental results are discussed.

©2010 Optical Society of America

OCIS codes: (060.2310) Fiber optics; (100.3175) Interferometric imaging; (140.3300) Laser beam shaping; (160.2290) Fiber materials; (220.4000) Microstructure fabrication.

References and links

1. C. Scott, Holswade, and F. M. Dickey, *Laser beam shaping* (CRC, 2005).
2. C. A. McQueen, J. Arlt, and K. Dholakia, "An experiment to study a nondiffracting light beam," *Am. J. Phys.* **67**(10), 912–915 (1999).
3. D. McGloin, and K. Dholakia, "Bessel beams: diffraction in a new light," *Contemp. Phys.* **46**(1), 15–28 (2005).
4. J. Arlt, V. Garcés-chavez, W. Sibbett, and K. Dholakia, "Optical micromanipulation using a Bessel light beam," *Opt. Commun.* **197**(4-6), 239–245 (2001).
5. K. S. Lee, and J. P. Rolland, "Bessel beam spectral-domain high-resolution optical coherence tomography with micro-optic axicon providing extended focusing range," *Opt. Lett.* **33**(15), 1696–1698 (2008).
6. S. Juodkazis, H. Misawa, and I. Maksimov, "Thermal accumulation effect in three-dimensional recording by picoseconds pulses," *Appl. Phys. Lett.* **85**(22), 5239–5241 (2004).
7. J. Durnin, J. J. Miceli, Jr., and J. H. Eberly, "Diffraction-free beams," *Phys. Rev. Lett.* **58**(15), 1499–1501 (1987).
8. Y. Lin, W. Seka, J. H. Eberly, H. Huang, and D. L. Brown, "Experimental investigation of Bessel beam characteristics," *Appl. Opt.* **31**(15), 2708–2713 (1992).
9. G. Indebetouw, "Nondiffracting optical fields: some remarks on their analysis and synthesis," *J. Opt. Soc. Am. A* **6**(1), 150–152 (1989).
10. S. K. Mohanty, K. S. Mohanty, and M. W. Berns, "Organization of microscale objects using a microfabricated optical fiber," *Opt. Lett.* **33**(18), 2155–2157 (2008).
11. J. K. Kim, J. Kim, Y. Jung, W. Ha, Y. S. Jeong, S. Lee, A. Tünnermann, and K. Oh, "Compact all-fiber Bessel beam generator based on hollow optical fiber combined with a hybrid polymer fiber lens," *Opt. Lett.* **34**(19), 2973–2975 (2009).
12. J. F. Michel, Dignonnet, *Rare-earth-doped fiber lasers and amplifiers* (Marcel Dekker, 2001).
13. K. Oh, S. Choi, Y. Jung, and J. W. Lee, "Novel Hollow Optical Fibers and Their Applications in Photonic Devices for Optical Communications," *J. Lightwave Technol.* **23**(2), 524–532 (2005).
14. S. Monk, J. Arlt, and M. J. Padgett, "The generation of Bessel beams at millimeter-wave frequencies by use of an axicon," *Opt. Commun.* **170**(4-6), 213–215 (1999).
15. X. Zhu, A. Schülzgen, H. Li, H. Wei, J. V. Moloney, and N. Peyghambarian, "Coherent beam transformations using multimode waveguides," *Opt. Express* **18**(7), 7506–7520 (2010).
16. X. Tsampoula, K. Taguchi, T. Čizmar, V. Garcés-Chavez, N. Ma, S. Mohanty, K. Mohanty, F. Guun-Moore, and K. Dholakia, "Fiber based cellular transfection," *Opt. Express* **16**(21), 17007–17013 (2008).

1. Introduction

Laser beam shaping [1] has recently received intense attention in atomic physics and nano-bio science as well as ultra high-precision laser processing. Especially Bessel beams or Bessel-like beams have been on the center of focus for their unique non-diffracting and self-reconstructing nature, which were not attainable in conventional Gaussian beam optics limited by the classical Rayleigh range [2,3]. The Bessel beams have enabled new novel scientific investigations such as longitudinal optical trapping of multiple mesoscopic particles along the axial direction [4], high resolution optical coherence tomography over a large depth [5], and three-dimensional nano-micro processing [6] to name a few. Since J. Durnin's first experimental demonstration of Bessel beam using an annular ring aperture placed at the back focal plane of a convex lens [7,8], majority of Bessel beam related reports have been based on macroscopic optical elements whose typical size ranged from millimeters to centimeters. Among them, a conical shaped refractor called as an axicon [3,9] has been the key optical element in recent Bessel beam generation (BBG) research, where the incident plane wave forms a concentric interference pattern similar to a Bessel function, $J_0(x)$, by its conical surface.

Recently novel attempts have been reported using fiber optics for BBG [10,11] to provide an integrated micro-solution, which is inherently compatible to rapidly developing rare earth ion doped fiber lasers [12]. A single mode fiber end has been chemically etched to form a conical-shaped axicon at the fiber tip [10], but its non-diverging length was very limited in comparison to bulk counterpart. Recently the authors have reported a novel composite optical fiber BBG device in the visible lasers with a non-diffracting length over 1 mm comparable to bulk axicons [11]. The device structure was fiber optic analogue of Durnin's method [7,11] showing a strong potential for compact and integrated micro BBG device, but it required a special hollow optical fiber [13] along with optimized splice conditions, and a separate post-process to form a polymeric lens.

In this study we report a new type of novel all-fiber BBG device fully compatible to Yb-doped fiber laser at the wavelength of 1.08 μm providing an integrated all-fiber micro-solution for laser beam shaping, for the first time. We successfully demonstrated two-dimensional optical trapping and transport of multiple dielectric particles along the axial direction to confirm both non-diffracting and self-reconstructing natures of the Bessel-like beam.

2. Theoretical base and fabrication of all-fiber BBG

Bessel beam is a particular solution of Helmholtz wave equation for a monochromatic wave as in Eq. (1). Its propagation along the axial direction, z , is decoupled from the extension of the wave in the transverse plane as in Eq. (2) [3,7].

$$(\nabla^2 + k^2)\Phi(x, y, z; \kappa) = 0. \quad (1)$$

$$\Phi_B(x, y, z; \kappa) = J_0(\alpha\rho) e^{i\beta z}. \quad (2)$$

The solution includes $J_0(x)$, zeroth-order Bessel function, where $\alpha^2 + \beta^2 = \kappa^2$, $x^2 + y^2 = \rho^2$. The Bessel function results in a concentric ring intensity pattern and its central peak plays the major role to provide the gradient force for optical trapping of dielectric particles [4]. Bessel-like beams generated by bulk axicons maintain the focused central spots along the axial direction over several millimeters, which is dependent upon the cone angle, radius, and the refractive index of the axicon [14]. Alignment of the incident laser beam along the axicon axis, whose diameter is 50~100 mm [14], has been a critical issue and highly stabilized beam steering systems have been required.

Despite very successful implementation of bulk axicon in BBG, its large form factor and tight alignment tolerance has become a major bottleneck for further micro-nano scale applications such as in-vivo investigations of nano-bio particles. Therefore, alignment-free

micron-scale integrated BBG device would open a new avenue of optical trapping applications in the emerging nano-bio science.

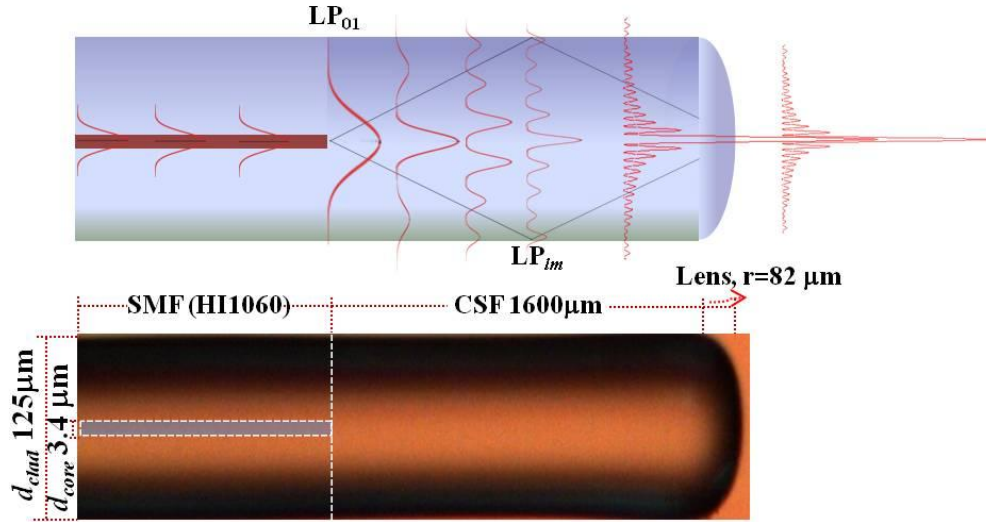


Fig. 1. (a) Schematic diagram of the principle of Bessel-like beam generation in the proposed all-fiber BBG device by multi-mode interference. (b) Photographic image of the fabricated all-fiber BBG and its geometrical parameters.

The schematic structure of the proposed BBG is shown in Fig. 1. It is composed of three fiber segments serially concatenated: single mode fiber (SMF, Corning HI-1060), coreless silica fiber (CSF) drawn from a pure silica glass rod, and micro-lens formed at the end-facet of CSF. As in Fig. 1(a), the fundamental LP_{01} mode from the input SMF excites LP_{0m} higher order modes in CSF. In the multi-mode interference (MMI) theory, these excited modes can form a basis set to form an arbitrary field distribution E_{out} as they propagate [15].

$$E_{out}(r, \varphi, l) = \sum_{m=1} C_m e_m(r, \varphi) e^{-i\beta_m l} \quad (3)$$

Here $e_m(r, \varphi)$ is the electric field of the LP_{0m} modes excited along CSF, with their amplitudes of C_m and the propagation constants of β_m . l is the length of CSF. In this study, we used CSF whose diameter was $125 \mu\text{m}$ and the surrounding air served as the cladding to allow significantly larger number of excited modes enough to obtain Bessel-like field distribution in comparison to conventional multimode fibers whose core diameter are in the range of $50\text{--}62.5 \mu\text{m}$. The excited symmetric modes propagate along the CSF accumulating the phase differences to form a concentric intensity distribution similar to Bessel function by MMI at an optimal propagation length l of CSF. This concentric ring MMI pattern is then focused by integrated fiber lens formed at the end facet of the CSF to subsequently generate a Bessel-like beam. Note that the proposed device is based on MMI along the fiber and its imaging, in contrast to prior Fourier transformation techniques used in the ring apertures [7,11] and axicons [9].

A photograph of the fabricated device is shown in Fig. 1(b). The SMF provided the fundamental LP_{01} mode guidance for the incident Yb-doped fiber laser at the wavelength of $1.08 \mu\text{m}$ with the the mode field diameter of $\sim 4.3 \mu\text{m}$. The SMF had the LP_{01} mode cut-off near 920 nm and the relative core-cladding refractive index, Δ , was 1% . CSF was drawn from a fused silica rod to the cladding diameter of $125 \mu\text{m}$. The SMF and CSF were seamlessly connected by electric arc fusion splices. The fiber lens at the end of CSF was fabricated by applying an electric arc over the vertically cleaved end-facet of CSF. The high temperature of

the electrical arc melted the CSF, which flew over the CSF cross-section to form a convex lens. Note that all the constituents of the proposed device are centered along the fiber axis obviating tedious alignment efforts required in the conventional bulk axicons. It is also noteworthy that the device thickness is reduced to 125 μm , which can provide flexible and efficient maneuvering capability for in-vivo optical trapping applications.

3. Simulation based on MMI theory

The evolution of the light intensity pattern from the incident LP_{01} mode in the SMF along the CSF, and through the fiber lens was numerically investigated using a beam propagation method (BPM) package. The most critical parameters for Bessel-like beam generation were: the radius of the fiber lens, r_{lens} , the CSF diameter, d_{CSF} , and the CSF length, l_c , which directly affected the non-diffracting length, Z_{max} , central beam intensity, and central peak diameter of the output beam. After manipulating all these parameters, we discovered geometric optimization for Bessel-like beam generation, where r_{lens} is near 80 μm and d_{CSF} is 125 μm .

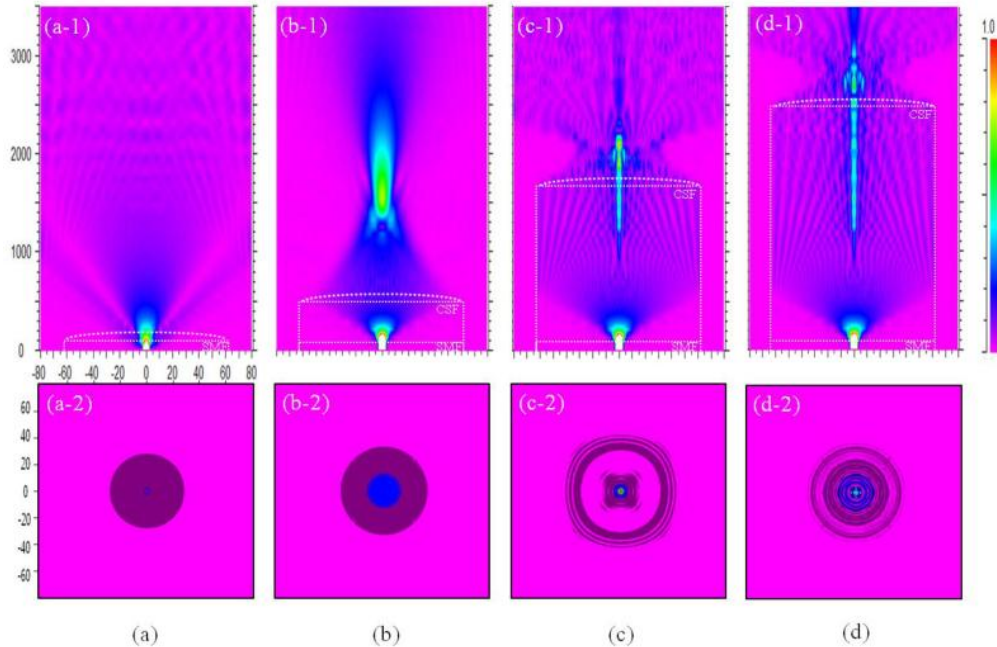


Fig. 2. Beam Propagation Method (BPM) simulation results for the proposed devices with various CSF lengths. The upper row shows the longitudinal intensity distribution along the z -axis, and the lower row shows the maximum intensity distribution measured at 300 μm apart from fiber facet in the transverse x - y plane. The SMF end facet is at $z=100 \mu\text{m}$ and the CSF and fiber lens ($r_{\text{lens}}=82 \mu\text{m}$) are overlaid in white dashed lines. The CSF lengths are (a) $l_c=0$, (b) 400 μm , (c) 1600 μm , (d) 2400 μm .

The results of parametric optimization are summarized in Fig. 2 and we assumed the incident wavelength, λ_{in} of 1.08 μm , r_{lens} of 82 μm and d_{CSF} of 125 μm . Here we assumed the refractive index outside the fiber was 1.33 because the device was immersed in the water for the optical trapping experiments, which will be discussed in the next section. For various CSF lengths, the intensity profiles along the longitudinal z -direction and in the transverse x - y plane are presented in the upper row and lower row, respectively in Fig. 2. For the case of $l_c=0 \mu\text{m}$ as in Fig. 2(a) where the CSF was absent, the output beam rapidly diverged similar to Gaussian beam. As the CSF length increased, concentric ring patterns began to appear from the circumference toward the center as in Fig. 2(b), (c), and (d). In the BPM analysis, we found that the optimal l_c was 1600 μm , which showed the longest non-diffracting length

($Z_{\max} \approx 500 \mu\text{m}$) along with Bessel-like concentric intensity pattern. Note that the optimal condition also provided the most stable central beam intensity distribution and central peak diameter along the z-axis.

4. Experiment results

-Beam intensity distribution of transverse and longitudinal plane

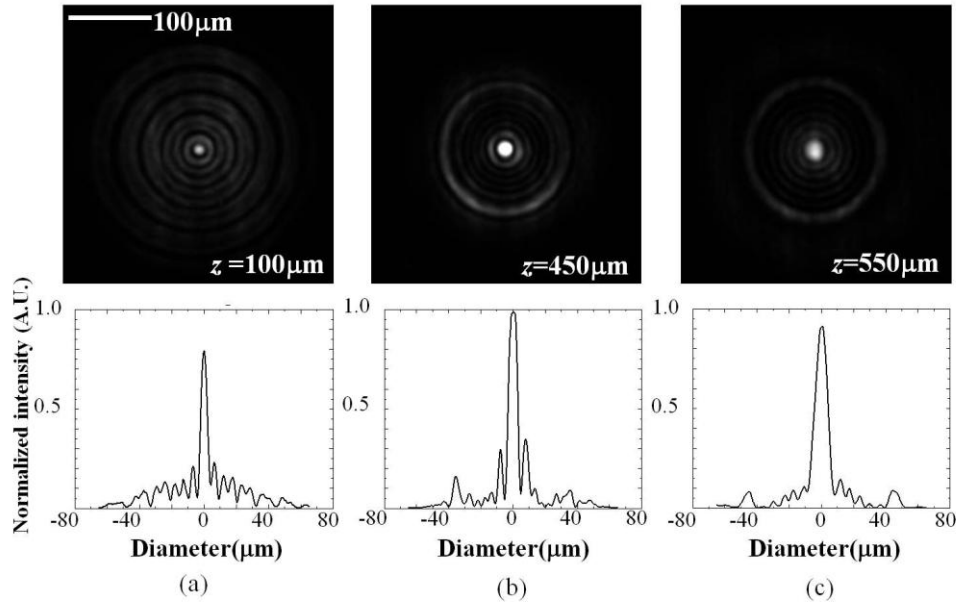


Fig. 3. Intensity distributions for the beam from the fabricated all-fiber BBG device, measured by CCD camera. The CSF length was $l_c=1600 \mu\text{m}$ and the axial position was (a) $z=150 \mu\text{m}$, (b) $450 \mu\text{m}$, (c) $550 \mu\text{m}$.

Based upon numerical analysis, we fabricated proposed BBG devices with three different CSF lengths, $l_c=400$, 1600 , and $2400 \mu\text{m}$. The radius of curvature of the fiber lens was set to $82 \mu\text{m}$ by optimizing the arc-conditions. A picture of the fabricated device is shown in Fig. 1(b) along with its geometrical parameters. A continuous wave (CW) Yb-doped fiber laser ($\lambda_{in}=1.08 \mu\text{m}$) was used as a light source, whose laser cavity was closed by fiber Bragg grating and pumped by fiber coupled 910 nm laser diodes. The input optical power of the laser was 89.52 mW and the output power of the device was 81.13 mW , which corresponds to a low insertion loss of 0.42 dB .

In order to confirm the Bessel-like beam pattern, we measured the cross-sectional intensity distributions of the output beam using an infrared CCD camera (Edmund eo1312) at every $50 \mu\text{m}$ along the z axis. For precise measurements, the proposed device was mounted on an electro-mechanical translation system with the position control accuracy of $0.1 \mu\text{m}$. The measured intensity patterns are summarized in Fig. 3 for the axial distances of 100 , 450 , and $550 \mu\text{m}$. The images in the upper row of Fig. 3 clearly show Bessel-like beam characteristics with the central spike surrounded by concentric ring intensity patterns, which showed a good agreement with numerical analysis in Fig. 2(c) for $l_c=1600 \mu\text{m}$. The line profiles of the measured intensity distributions are shown in the lower row of Fig. 3, which also confirmed that the output beam can be well approximated to the zero-th order Bessel function. It was also noted that this Bessel-like beam intensity distribution remained over the axial distance of $500 \mu\text{m}$ as predicted by BPM in Fig. 2(c).

To confirm the non-diffractive nature of the Bessel-like beam from the proposed device, we further measured the variations in the intensity at the central peak and its full width at half

maximum (FWHM) diameter along the axial direction. The experimental measurements are summarized in Fig. 4.

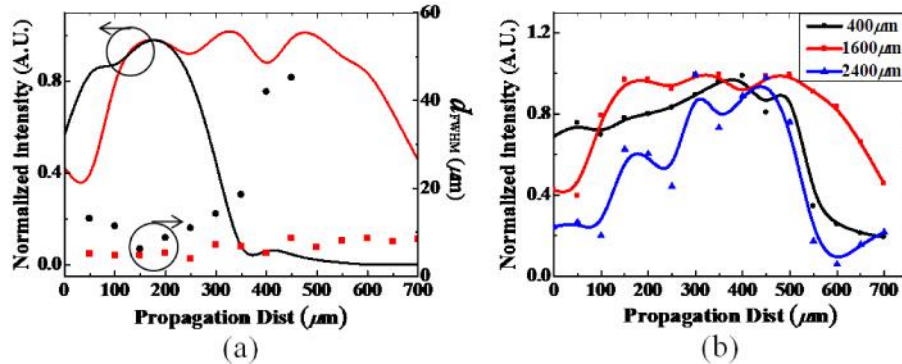


Fig. 4. (a) The central peak intensity profile along the longitudinal direction for the proposed device (red line) and vertically cleaved SMF (black line). The right axis is the FWHM diameter, d_{FWHM} . Red squares are for the proposed device and black circles are for SMF. (b) longitudinal intensity distribution for the proposed devices with various CSF lengths.

The output beam of the proposed device, the red line, maintained its peak intensity over the axial distance of 500 μm in Fig. 4(a). In contrast, the axial power from the cleaved conventional SMF rapidly decreased due to its diffracting nature as in black line. Within the non-diffracting length, the proposed device shows the average FWHM beam diameter, d_{FWHM} of 6.44 μm ranging from the minimum of 3.89 μm at the focal plane of fiber lens around $z = 250 \mu\text{m}$ to the maximum of 8.57 μm at $z = 600 \mu\text{m}$. See the red squares in Fig. 4(a). The axial intensity distributions of the fabricated devices with various CSF lengths are shown in Fig. 4(b). For the CSF length of $l_c = 400 \mu\text{m}$, the device showed a shorter non-diffracting length of $\sim 400 \mu\text{m}$. In the case of 2400 μm long CSF, the axial intensity showed a large fluctuation with an abrupt decrease over the axial position of 500 μm . The device with the optimal CSF length near 1600 μm showed the most stable and longest non-diffracting length, which is in a good agreement with the numerical prediction in Fig. 3.

-Optical trapping and transport of multiple dielectric particles

As a final step to validate the self re-construction nature of the Bessel-like beam from the proposed device, we carried out optical trapping experiments using polystyrene dielectric beads. A micro channel with 200 μm width 200 μm height for was devised for the fiber BBG device and the channel was connected to a circular reservoir that contained a milk-water suspension [11] and 10 μm diameter polystyrene beads with the refractive index $n_b = 1.55$. The non-diffracting beam silhouette from the proposed device was clearly observed by the scattering in the colloidal solution as in Fig. 5(a). Using a CCD camera mounted on an inverted microscope, we could successfully observe optical trapping and subsequent transport of the dielectric beads along the axial direction in a real-time video (25 frame per second). Particles near the edge of the beam were trapped toward the center by the gradient force and transported along the axial direction by radiation scattering force. It is also observed that two beads marked by white arrows were simultaneously trapped along z axis as shown in Fig. 5(b), which directly confirms the self-reconstructing nature of the beam from the proposed device.

In comparison to prior fiber axicons [10], the proposed device can provide an order of magnitude longer non-diffracting length exceeding 500 μm , along which multiple particles can be trapped. Prior fiber axicons required optical power over 146mW [10], yet the proposed

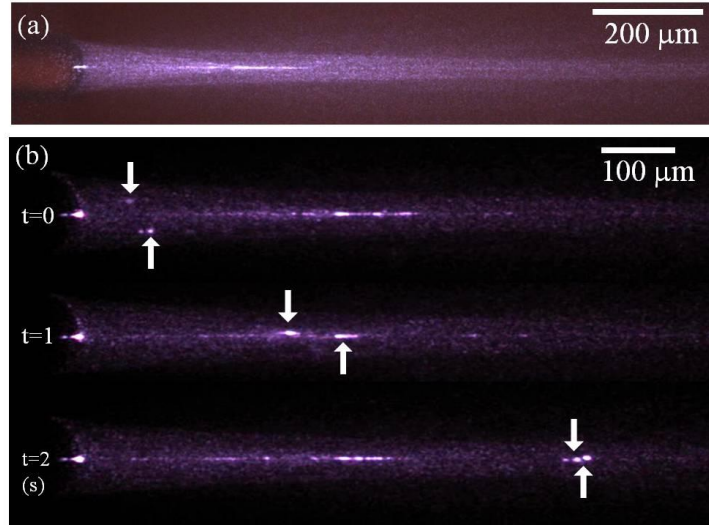


Fig. 5. (a) The image of Bessel-like beam propagation out of the proposed device in a colloidal solution. (b) Optical trapping of multiple dielectric particles (marked as white arrows) and subsequent optical transport along the axial direction.

device was operating normally at almost half of the power, 81.13 mW, providing more efficient and faster 2D optical trapping of dielectric particles.

Recently pulsed laser Bessel beams have been reported to take advantage of broadband supercontinuum source [16]. The proposed device would also allow pulsed laser operation if the the average power of pulsed laser fairly corresponds to that of CW lasers used in the experiment and the center wavelength of pulsed laser will be near to that of CW laser.

5. Conclusion

In summary, we successfully proposed and demonstrated a novel all-fiber device to generate a Bessel-like beam based upon multimode interference along the coreless silica fiber segment and subsequent focusing its concentric ring pattern using a fiberized lens. Non-diffracting nature of the beam was predicted for an optimal coreless fiber length of 1600 μm and fiber lens radius of 82 μm . Experimentally the non-diffracting length over 500 μm with a low insertion loss of 0.42 dB was achieved for Yb-doped fiber laser at the wavelength of 1.08 μm , showing a good agreement with theoretical predictions. Self re-construction nature of the beam was also experimentally confirmed by trapping of multiple polystyrene beads of 10 μm diameter, and their transport along the axial direction. The proposed all-fiber device can be a very attractive alternative to conventional bulk optics to generate the Bessel-like beams opening new applications requiring an in situ compact integrated solution in optical manipulation of nano-meso-scopic particles can be readily applied in novel nano- and micro-pattern generation.

Acknowledgments

This work was supported in part by the NRF under Grant ROA-2008-000-20054-0, Grant R15-2004-024-00000-0, Grant 2009-8-2175, and Grant 2010-8-0939, Grant 2010-8-0037 (the European Community's Seventh Framework Program [FP7/2007-2013] under Grant agreement no 219299, Gospel), Grant 2009-8-1339, Grant 2009-0093823, and in part by the Brain Korea 21 Project of the KRF.